



Ectopic activation of GABA_B receptors inhibits neurogenesis and metamorphosis in the cnidarian *Nematostella vectensis*

Shani Levy¹, Vera Brekhman¹, Anna Bakhman², Assaf Malik¹, Arnau Seb -Pedr s³, Mickey Kosloff² and Tamar Lotan¹

The metabotropic gamma-aminobutyric acid B receptor (GABA_BR) is a G protein-coupled receptor that mediates neuronal inhibition by the neurotransmitter GABA. While GABA_BR-mediated signalling has been suggested to play central roles in neuronal differentiation and proliferation across evolution, it has mostly been studied in the mammalian brain. Here, we demonstrate that ectopic activation of GABA_BR signalling affects neurogenic functions in the sea anemone *Nematostella vectensis*. We identified four putative *Nematostella* GABA_BR homologues presenting conserved three-dimensional extracellular domains and residues needed for binding GABA and the GABA_BR agonist baclofen. Moreover, sustained activation of GABA_BR signalling reversibly arrests the critical metamorphosis transition from planktonic larva to sessile polyp life stage. To understand the processes that underlie the developmental arrest, we combined transcriptomic and spatial analyses of control and baclofen-treated larvae. Our findings reveal that the cnidarian neurogenic programme is arrested following the addition of baclofen to developing larvae. Specifically, neuron development and neurite extension were inhibited, resulting in an underdeveloped and less organized nervous system and downregulation of proneural factors including *NvSoxB(2)*, *NvNeuroD1* and *NvElav1*. Our results thus point to an evolutionarily conserved function of GABA_BR in neurogenesis regulation and shed light on early cnidarian development.

Gamma-aminobutyric acid (GABA), the major inhibitory neurotransmitter in both vertebrates and invertebrates, plays a key role in modulation of neuronal activity. GABA activity is mediated by two distinct receptors, the ionotropic GABA_A and the metabotropic GABA_B. The GABA_A receptor is a chloride ion channel that mediates fast synaptic inhibition, while the GABA_B receptor (GABA_BR) is a G protein-coupled receptor (GPCR) that produces prolonged and slow synaptic inhibition via second messengers and modulation of calcium (Ca²⁺) and potassium (K⁺) channels¹. GABA_BR is an obligatory heterodimer comprising GABA_{B1}R and GABA_{B2}R subunits^{2–4}. GABA binds to a large Venus flytrap (VFT) domain in the extracellular portion of GABA_{B1}R^{3,6}, whereas GABA_{B2}R activates the coupled G protein and enhances ligand affinity via interactions with GABA_{B1}R^{4,7–11}. During mammalian embryonic development, GABA_BR plays important roles in neuronal proliferation, migration and network formation^{12–15}, while in adults it inhibits neuronal differentiation and controls stem and progenitor cell proliferation^{16,17}.

Although GABA_B receptors have been extensively studied in mammals, *Drosophila* and *Caenorhabditis elegans*^{18–21}, little is known of their function in non-bilaterian animals. Cnidaria are the phylogenetic sister group to Bilateria and one of the earliest-branching metazoan taxa to possess a nervous system²². Other early metazoans, such as Placozoa and Porifera, contain genes related to sensory transmission yet lack neurons and synapses, while Ctenophora harbour a nervous system of unclear homology to the cnidarian and bilaterian systems^{23–25}. Moreover, this lineage is lacking most of the classical neurotransmitters found in Bilateria, including GABA²⁶. The cnidarian diffuse nervous system contains three primary types of neuronal cell: sensory neurons, ganglion neurons and cnidocytes

(the stinging cells that characterize the phylum)^{27–30}. Their phylogenetic position and simple nerve-net structure make Cnidaria an attractive model for the exploration of basic neurogenic processes.

Among cnidarians the sea anemone *Nematostella vectensis* has become an important model system, with a published genome^{30–32}. During its simple life cycle, an embryo develops into the larval stage of a swimming planula, which metamorphoses into a primary polyp that eventually gives rise to the mature polyp³³. Despite its relatively simple body plan, analysis of the *Nematostella* genome has revealed an unexpected complexity and extensive conservation of vertebrate genomic content and organization³². This similarity is also reflected in a conserved neuronal gene repertoire, which includes orthologous genes associated with cholinergic, glutamatergic and aminergic neurotransmission^{27,34–37}. Genes putatively related to GABA signalling were identified in *Nematostella* using large-scale phylogenetic analysis³⁴. GABA itself was shown to accumulate early in *Nematostella* planulae at the aboral pole and in ectodermal neurons³⁶. Nevertheless, the role of GABA during development or in neurogenesis is unknown, and the receptors that mediate GABA signalling remain uncharacterized.

Here, we identified four putative GABA_{B1}R genes in *Nematostella* containing extracellular domains with a predicted three-dimensional (3D) structure similar to mammalian GABA_{B1}R, including conserved residues that mediate agonist binding. Using baclofen, a clinically employed GABA_{B1}R-specific agonist, we elucidated the role of GABA-mediated signalling during early *Nematostella* development. We found that baclofen inhibited neurogenesis, reversibly arresting planula-to-polyp transformation. These results suggest a conserved role for GABA signalling in the control of neuronal network formation in the sea anemone, and open new avenues for the study

¹Marine Biology Department, The Leon H. Charney School of Marine Sciences, University of Haifa, Haifa, Israel. ²Department of Human Biology, University of Haifa, Haifa, Israel. ³Centre for Genomic Regulation, Barcelona Institute of Science and Technology, Universitat Pompeu Fabra, Barcelona, Spain. ✉e-mail: kosloff@sci.haifa.ac.il; lotan@univ.haifa.ac.il

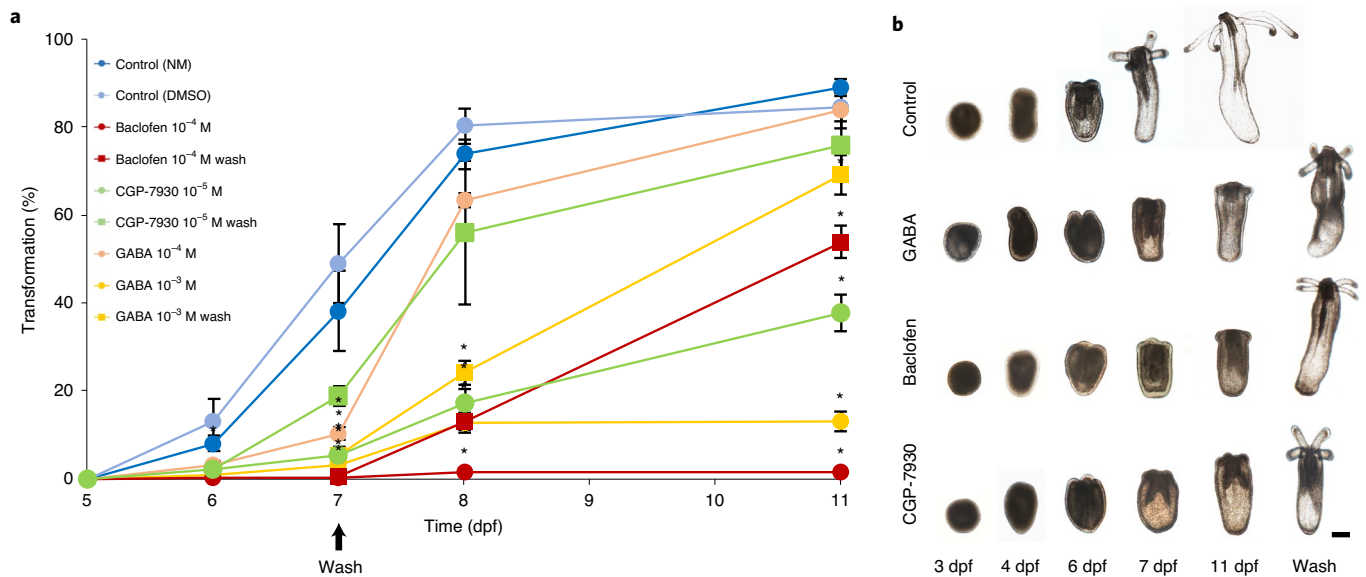


Fig. 1 | GABA and a specific GABA_BR agonist and modulator cause reversible inhibition of *Nematostella* metamorphosis. **a, Percentage of planulae that transformed into polyps as a function of time (dpf) in controls (NM (*Nematostella* medium), DMSO) and in planulae treated with GABA (10⁻³, 10⁻⁴ M), the GABA_BR agonist baclofen (10⁻⁴ M) or the positive GABA_{B2}R allosteric modulator CGP-7930 (10⁻⁵ M). Controls and agonists (circles) were added at 3 dpf. At 7 dpf, agonists were removed in half of the samples (rectangles). The results are presented as the average percentage transformation ± s.e.m. Asterisks indicate significant differences from the control ($P < 0.05$, t -test). **b**, Planula development and metamorphosis under control conditions and following treatment with GABA, baclofen or CGP-7930. Note that treated planulae were smaller and failed to metamorphose, whereas control planulae transformed into primary polyps as early as 7 dpf. Four days after removal of compounds, planulae recovered and transformed into primary polyps (wash, 11 dpf). Scale bar, 100 μm.**

of molecular mechanisms underlying basic metamorphic processes across evolution.

Results

GABA_B receptors play a role in planula-to-polyp transformation. The morphogenetic transition of *Nematostella* planulae into primary polyps occurs 7–12 days post fertilization (dpf). During this transition, the planulae cease active swimming, settle and the four tentacle buds elongate. Since GABA was found to accumulate in early *Nematostella* planulae³⁶, we tested the effect of GABA on planula-to-polyp transformation. We found that the addition of GABA (10⁻³ M) at 3 dpf, in the early planula stage, prevented metamorphosis of >85% of the planulae while about 80% of control planulae metamorphosed by 8 dpf (Fig. 1a). A lower GABA concentration (10⁻⁴ M) reduced the rate of metamorphosis but did not inhibit the process, probably due to natural GABA degradation (Fig. 1a). Arrested planulae continued to develop to the late planula stage, developing primary mesenteries, pharynx and initial tentacle buds similarly to untreated planulae, but their development was much slower (Fig. 1b).

To identify which GABA receptor family is involved in the inhibition of transformation, we tested the effects of GABA_AR and GABA_BR agonists. The GABA_AR agonist muscimol (10⁻⁴ M) demonstrated toxic and lethal effects, preventing further development of early planulae, while the GABA_{B1}R agonist baclofen (10⁻⁴ M), a highly specific stereo-GABA_{B1}R agonist, yielded physiological effects similar to GABA but inhibited metamorphosis to a greater degree (Fig. 1a). Additionally, CGP-7930, a GABA_{B2}R positive allosteric modulator³⁸, prevented metamorphosis in >60% of planulae, with affected planulae presenting a morphology similar to that of GABA- or baclofen-treated planulae (Fig. 1b). Agonist-treated planulae did not transform into primary polyps, their tentacle buds did not develop and their body structure, marked by F-actin, displayed a pattern similar to that of control (untreated) late planulae

before metamorphosis (Fig. 1b and Extended Data Fig. 1). Treated and control planulae exhibited a similar apical tuft, an organ that characterizes the planula stage and is lost during metamorphosis (Extended Data Fig. 1). Because oralization and tentacle induction are controlled by the Wnt pathway^{39,40}, we tested the expression of specific Wnt ligands characterizing the oral pole of *Nematostella* planulae⁴¹. We found that expression levels and localization did not change following baclofen treatment (Supplementary Fig. 1), suggesting that Wnt ligand expression does not mediate the inhibitory effect of GABA_BR signalling.

The effects of GABA, baclofen and CGP-7930 were reversible—removal of these compounds at 7 dpf restored metamorphosis and enabled the planulae to develop into primary polyps (Fig. 1a). However, addition of GABA_BR antagonists such as saclofen, phaclofen or CGP 54626 had no detectable effect on planula development or metamorphosis rate. These results suggest that a GABA_BR homologue, which is resistant to known antagonists, mediates the effect of GABA on planula-to-polyp transformation.

Characterization of *Nematostella* GABA_B receptors. We identified eight candidate GABA_BR homologues in *Nematostella* (Methods) containing the conserved extracellular N-terminal GABA-binding VFT domain and the seven transmembrane domains characteristic of GPCRs⁴² (Extended Data Fig. 2). However, the intracellular C-terminal domains, which were suggested as non-essential for functional GABA_BR heterodimers^{42–45}, show low similarity in *Nematostella* homologues. This suggests that GABA_BR C termini can differ dramatically between mammals and cnidarians without affecting essential functions.

To test whether the identified GABA_BR homologues exhibit neuronal-related expression, we quantified their single-cell expression by searching the recently published *Nematostella* cell-type expression atlas⁴⁶ (Supplementary Fig. 3). Indeed, five of the homologues (MH194577, MH194579, v1g244104, v1g239821 and

v1g206093) were expressed in neuronal cell clusters, including in larval neurons. Conversely, the expression of v1g243252, mainly in adult digestive filaments, together with its divergent protein architecture (Extended Data Fig. 2), suggested that this homologue does not mediate the observed phenotypes.

We compared the extracellular domains of *Nematostella* and bilaterian homologues (Fig. 2 and Supplementary Fig. 2). Only four sequences presented both the homologous 3D scaffold structure and the conserved residues needed for agonist binding, while the other four sequences either lacked essential structural and binding residues or included an insertion predicted to interfere with agonist binding. In vertebrate GABA_{B1}R, the extracellular VFT domain consists of two lobe-shaped domains (LB1 and LB2) that close following ligand binding. This structure is stabilized by two conserved disulfide bridges that are essential for GABA binding⁶. MH194577–79, MH355581 and v1g244104 contain corresponding cysteines while v1g239821, v1g206093 and v1g243252 do not; the latter are thus predicted not to bind GABA (Fig. 2 and Supplementary Fig. 2). Similarly, MH194577–79 and MH355581 contain residues that are similar to critical GABA-binding-site positions in human GABA_{B1}R^{5,6}, whereas in v1g244104 an arginine that corresponds to Ser153 will interfere with agonist binding, suggesting that v1g244104 will not bind GABA or its analogues (Fig. 2). All *Nematostella* GABA_BR homologues contain two conserved tyrosine residues corresponding to Tyr250 and Glu349 that can support agonist binding (Fig. 2) while His170 is not conserved in *Nematostella*, suggesting that it is dispensable. Taken together, four *Nematostella* homologues (MH194577–79 and MH355581) contain functional GABA/baclofen-binding sites, suggesting that they are functional GABA_{B1}R homologues.

We also analysed the conservation of GABA_{B1}R residues shown to mediate specific antagonist binding to human GABA_{B1}R. Gly64, Ser154 and Val159 are conserved in all *Nematostella* homologues, but Ser131 is conserved only in MH194577 and is substituted by alanine in MH355581. Residues in *Nematostella* homologues that correspond to Met312 are not conserved, as was the entire LB1 loop (Fig. 2). Comparison of the extracellular domain of human GABA_{B1}R bound to the antagonist CGP 54626 (ref. ⁵) with the corresponding predicted 3D structure in *Nematostella* revealed that the first and fifth loops in the predicted LB1 are longer than the corresponding

loops in human GABA_{B1}R (Fig. 3). These loops most probably will substantially reduce the binding pocket in *Nematostella* homologues and, since GABA_{B1}R antagonists are larger than agonists, will probably prevent antagonist binding in *Nematostella*, consistent with our results.

To test the roles of the identified GABA_{B1} receptors, we performed genetic perturbations using a recently published method for short hairpin RNA knockdown in *Nematostella*^{47,48}. We quantified the effects of shRNA knockdown by quantitative PCR along planula development and metamorphosis at 2–7 dpf. While the RNA levels of the tested genes were initially reduced, by 4 dpf and subsequently they had returned to control levels (Supplementary Figs. 4 and 5), showing that this method is not applicable for genes such as GABA_{B1}R that are expressed and function after 4 dpf.

Transcriptome analysis following GABA_BR activation. To identify genes and pathways involved in GABA_BR signalling and baclofen-mediated inhibition of metamorphosis, we took a whole-transcriptome RNA-sequencing approach. We analysed samples from planulae at different time points (2, 24 and 48 h after the addition of baclofen) at 4–6 dpf, just before metamorphosis

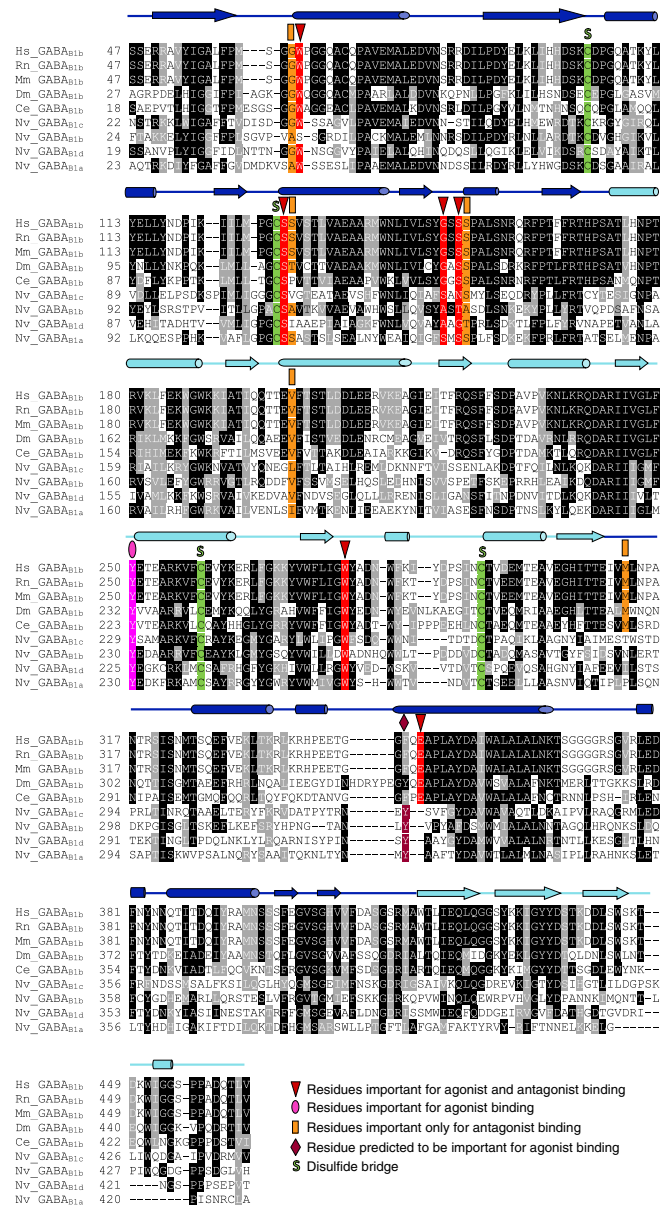


Fig. 2 | Sequence comparison of the extracellular regions in bilaterian and putative *Nematostella* GABA_{B1}R homologues. Identical residues are shaded black, and conservatively substituted residues grey. Residues involved in both agonist and antagonist binding are shaded red, those involved in agonist binding per se are magenta, those predicted to be involved in antagonist binding are Bordeaux and those involved in antagonist binding per se are shaded orange. Cysteines that were shown to form disulfide bridges (S) that stabilize the VFT domain and are critical for GABA binding (Cys103–129 and Cys259–293) are shaded green. The γ -amino group of agonists, including GABA and baclofen, form hydrogen bonds with Tyr250 in LB2 and with His170 and Glu349 in LB1. All *Nematostella* GABA_BR homologues contain a tyrosine residue in the corresponding position to Tyr250, and present a conserved tyrosine residue that 3D modelling showed could substitute for Glu349. His170 is not found in any *Nematostella* GABA_B homologue and is predicted to be dispensable for agonist binding. Secondary structure elements of human GABA_{B1}R are displayed above the alignment: α -helices are shown as cylinders and β -strands as arrows, shaded purple and cyan in the LB1 and LB2 subdomains of the extracellular VFT domain, respectively. Bilaterian sequence accession numbers: human (Hs), NP_068703; rat (Rn), AAD19657; mouse (Mm), AAH56990; *Drosophila* (Dm), AAF53431; *C. elegans* (Ce), ACE63490; and *Nematostella* (Nv) sequences: Nv_GABA_{B1a}, MH194577; Nv_GABA_{B1b}, MH194578; Nv_GABA_{B1c}, MH194579; Nv_GABA_{B1d}, MH355581.

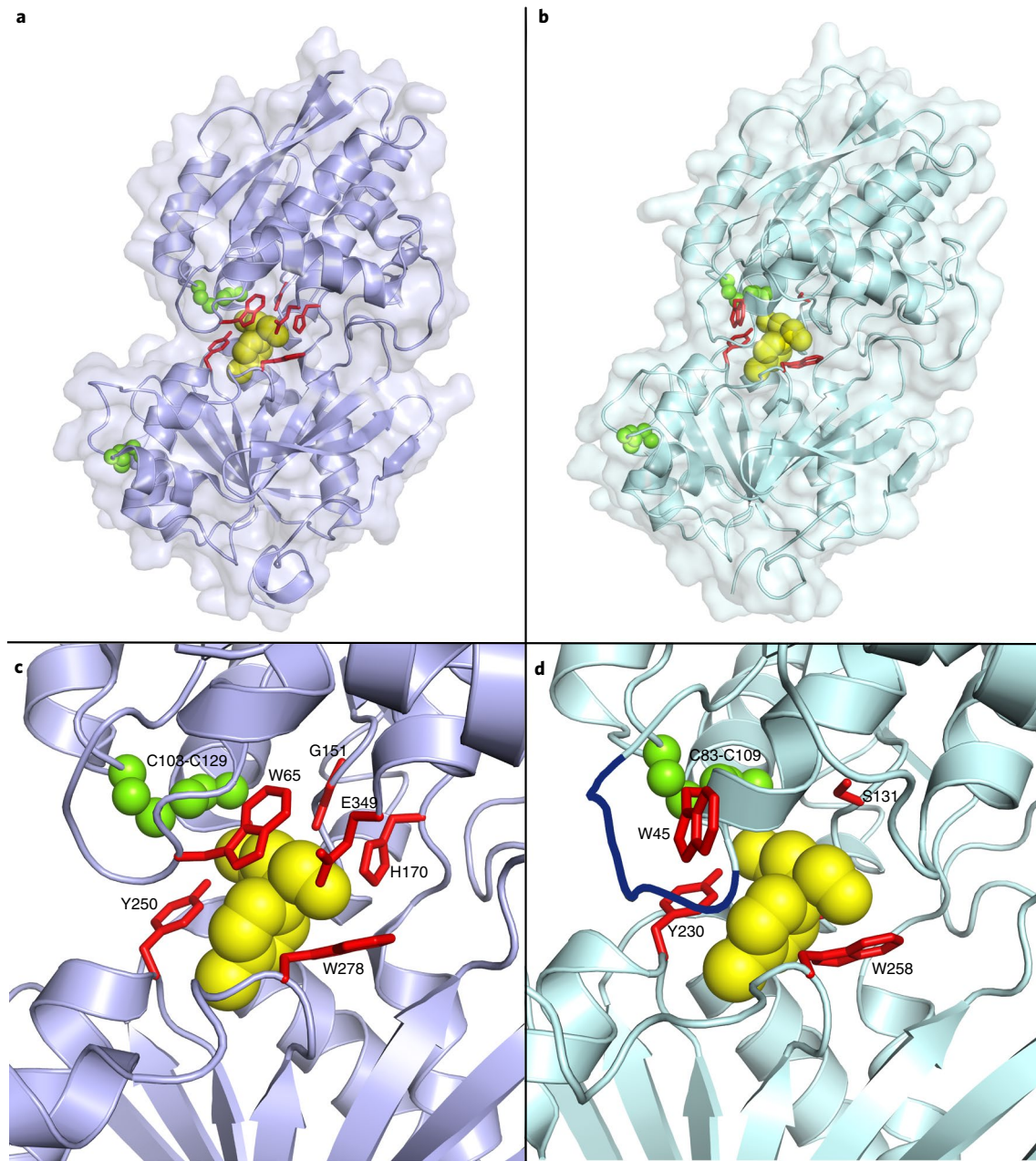


Fig. 3 | Three-dimensional visualization of the human and *Nematostella* GABA_BR extracellular region bound to baclofen. **a, The crystal structure of the extracellular VFT domain of the human GABA_{B1b} receptor (PDB ID 4MS4). **b**, A model of the corresponding extracellular domain in *Nematostella* (GABA_{B1a} MH194577), built with SWISS-MODEL using the human GABA_{B1b}R structure as template. **c**, The GABA-binding pocket in human GABA_{B1b}R. Residues participating in agonist binding are shown as red sticks, baclofen as yellow spheres and disulfide bridges as small green spheres. **d**, The predicted GABA-binding pocket in *Nematostella* GABA_{B1a}R. Conserved residues corresponding to GABA-binding sites in the human GABA_{B1b}R structure are shown as red sticks. Residues His170 and Glu349 in the human protein do not have corresponding residues in the *Nematostella* binding pocket. A longer loop in the *Nematostella* LB1 subdomain, which contains Met312 and is predicted to prevent binding of human GABA_{B1b}R antagonists, is shaded dark blue.**

begins (Fig. 4a). Because the effect of baclofen on planulae is reversible (Fig. 1), we also sampled planulae 2 and 24 h after removal of baclofen. In all treatments, >10,000 transcripts displayed significant yet corresponding changes in expression during development. Among these, the expression of 7,543 genes changed similarly during planula development (4–6 dpf) in both control and with baclofen treatment, while the expression of 3,852 genes changed only with baclofen treatment (Supplementary Table 1). To examine the effects over time we conducted non-metric multidimensional scaling analysis (nMDS) of the transcriptomic data, showing clear

differences between control and baclofen-treated planulae (Fig. 4b). Removal of baclofen had a dramatic effect within 2 h and, after an additional 24 h, the transcriptome of washed planulae further differed from both baclofen-treated and control planulae (Fig. 4b).

To demonstrate the specific effect of baclofen treatment, we compared expression at different time points using MA plot (mean of normalized counts versus log₂ fold changes) analysis (Fig. 4c,d), revealing three transcript groups. In the first, expression did not significantly differ between control and treated animals. In the second and largest group, transcript levels changed significantly

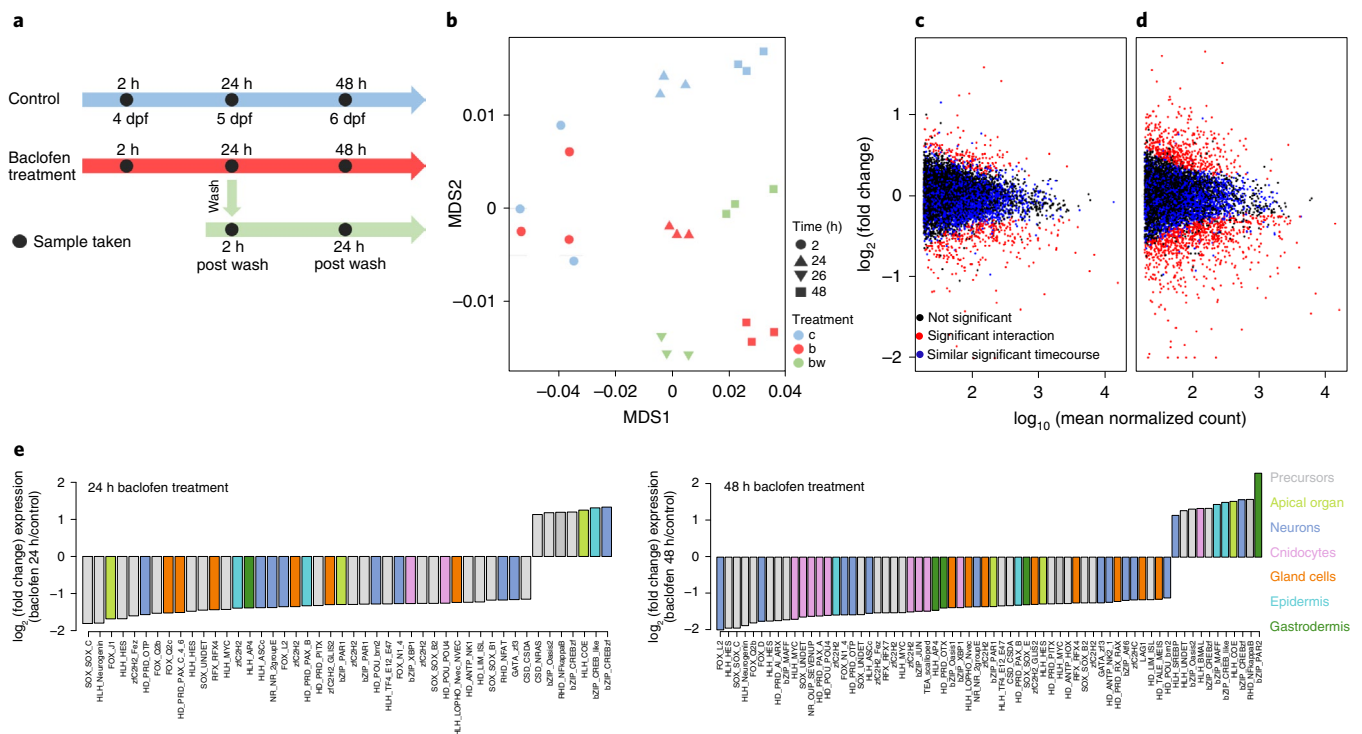


Fig. 4 | Transcriptomic analysis of control and baclofen-treated planulae. **a**, Schematic description of the experiment. Triplicate samples of control, baclofen-treated and baclofen-treated/washed planulae were taken at 4–6 dpf, 2, 24 or 48 h following baclofen addition. Twenty-four hours after the addition of baclofen, half of the treated planulae were washed and samples were taken 2 and 24 h post wash. **b**, nMDS analysis demonstrating the effect of baclofen (b) and baclofen wash (bw) on the planula transcriptome, relative to controls (c) ($k=2$ nMDS dimensions, stress = 0.08; see Methods). **c,d**, MA plot representation of gene expression fold changes at 24 versus 2 h (**c**) and 48 versus 2 h (**d**). Blue dots denote genes with significant time-dependent expression changes, regardless of baclofen treatment, and red dots denote genes for which baclofen significantly modulated the time-dependent effect (significant interactions, see Methods). Black dots denote genes with non-significant changes in expression. Negative log (fold change) values indicate inhibition. **e**, Cell-type-specific TFs affected by baclofen treatment, ordered by treatment/control log (fold change). TFs linked to progenitor/undifferentiated cells were mostly affected by baclofen (46% at 24 h, 36% at 48 h), followed by those associated with neuronal cell programmes (17% at 24 h, 18% at 48 h). Colours indicate the cell type in which the TF is expressed⁴⁶.

during development (at 24 and 48 h) in both groups, suggesting that baclofen treatment did not have a general inhibitory effect by inhibiting, for example, cell proliferation. The third group contained transcripts whose levels changed significantly following baclofen treatment.

We next compared control and baclofen-treated planulae at 4–6 dpf (2–48 h into the transcriptome experiment, respectively; Fig. 4a) using Gene Ontology (GO) enrichment analysis (Supplementary Table 2). While most downregulated processes (89% of the enriched GO terms) and upregulated processes (59%) were shared between baclofen-treated and control planulae, among the downregulated process we found no terms related to ‘cell proliferation’ or ‘cell death’. These findings suggest that baclofen treatment did not have a major effect on cell proliferation, nor arrest planula development.

Finally, to understand how cell-type identity programmes were affected by baclofen treatment, we searched for cell-specific transcription factors (TFs) as defined in the *Nematostella* cell-type expression atlas⁴⁶ (Fig. 4e). The majority of TFs affected by baclofen treatment were linked to progenitor/undifferentiated cells, including *SoxC*, *Hes* and *Myc*, followed by those associated with neuronal cell programmes such as *NeuroD1*, *FoxL2* and *AshA*. Overall, our analysis indicates that baclofen has a central effect on neuronal differentiation programmes.

Autoregulation of GABA biosynthesis. Since baclofen is not metabolized in the cell, we postulated that prolonged baclofen-mediated

activation of the GABA_BR pathway would reduce GABA biosynthesis. Therefore, we tested for changes in expression of putative homologues relevant to this pathway. Accordingly, expression of the presynaptic glutamate transporter homologues *EAAT1*, *EAAT3* and *EAAT5*, as well as that of four homologues of glutamic acid decarboxylases (*GADs*), which produce GABA, was downregulated in baclofen-treated planulae (Fig. 5a,b). Enzymes that degrade or re-uptake GABA from the synaptic cleft, such as GABA-transaminase (*GABA-T*), GABA transporter1 (*GAT1*) and inhibitory vesicle transporters (*vGATs*), were upregulated by baclofen. A second GABA transporter homologue, *GAT2*, was downregulated in baclofen-treated planulae. Interestingly, tumour susceptibility gene101 (*TSG101*), required for the endosomal transport complex and involved in GABA_BR degradation in vertebrates^{49–51}, was upregulated following the addition of baclofen and downregulated following its removal. Three GABA_A receptor subunits were also downregulated 48 h after baclofen treatment, as was one GABA_BR (v1g239821). However, expression levels of the other GABA_B subunits remained constant. The downregulation of GABA synthesis pathways and upregulation of GABA degradation pathways implies that GABA levels are reduced in baclofen-treated planulae. Indeed, we found strong GABA reduction in treated planulae (Fig. 5c,d). This suggests that, in the presence of functional GABA signalling and GABA regulatory pathways in *Nematostella*, baclofen activates a GABA_BR-dependent signalling pathway and triggers a specific autoregulation response that includes inhibition of GABA synthesis and enhanced GABA removal and degradation.

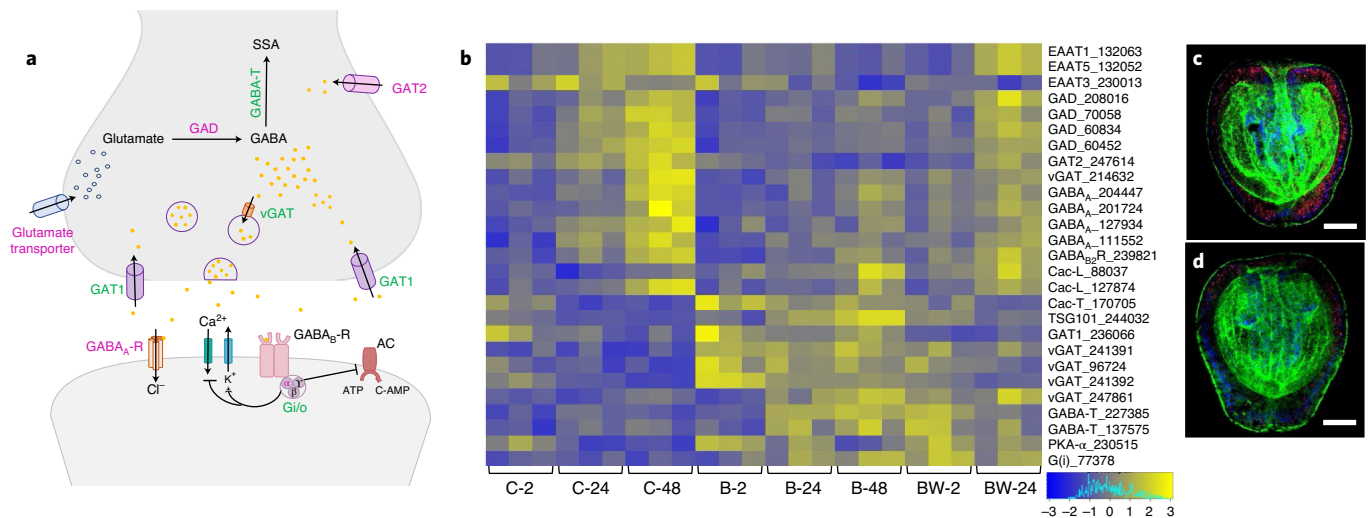


Fig. 5 | Autoregulation of GABA synthesis following baclofen treatment. **a**, Schematic illustration of the GABA pathway in the human synapse, based on ref. ⁹⁶. GABA is synthesized by decarboxylation of glutamate by GAD, is carried by vesicular GABA transporters (vGAT) into vesicles and, when released, it is taken up by high-affinity membrane transporters (GAT) into neurons and surrounding glia. There, it can either be recycled via the vesicular transporters or degraded by GABA-T to succinic semialdehyde (SSA). Post synaptically, GABA activates $GABA_B$ R, which in turn activates heterotrimeric G proteins from the $G_{i/o}$ subfamily ($G_{i/o}$) that inhibit adenylate cyclase (AC), thereby reducing cAMP levels in the cell. Transcripts up- or downregulated following baclofen treatment are coloured green and magenta, respectively. **b**, Heat map of transcript expression associated with GABA biosynthesis pathways as a function of time and treatment (C, control; B, baclofen treatment; BW, baclofen/wash). **c, d**, Confocal sections of control planulae (**c**) and planulae treated with baclofen for 48 h (**d**), labelled with antibodies against GABA (red), phalloidin (green) and DAPI (blue). The mean fluorescent intensity of GABA antibody staining was significantly different ($P < 0.001$) between control ($n = 19$) and baclofen-treated samples ($n = 22$). Scale bars, 50 μ m.

GABA signalling inhibits planula neurogenesis. Next, we examined the effect of $GABA_B$ R activation on early planula nervous system development. Transcriptomic analysis revealed significant downregulation of suggested proneural TFs, such as *NvSoxB(2)*^{52,53}, *NvAshA*⁵⁴, *NvAth-like*^{55–57}, *NvNeuroD1* (ref. ⁴⁶), *NvOtxB*⁵⁸, *NvSoxC*⁵⁵ and *NvBrn2* (ref. ⁴⁶), of two neuron-specific RNA-binding proteins, *NvElav1* (ref. ⁵⁹) and *NvMsi* (ref. ⁶⁰), and of other neuronal genes in baclofen-treated planulae (Fig. 4e and Supplementary Table 1). Spatial expression analysis of key neurogenic TFs in control and baclofen-treated planulae revealed that while their expression levels decreased, their expression patterns did not change (Fig. 6a,b). An exception to this downregulation trend was *NvSoxB1* (ref. ⁵²), which was initially downregulated in baclofen-treated planulae and then upregulated to an expression level similar to that of control (Fig. 6a,b).

We further tested a transgenic mOrange-expressing line under the control of *NvElav1* promoters⁵⁹. The addition of baclofen reduced *NvElav1* gene expression, resulting in a less organized neural net that lacked longitudinal neurons along the mesenteries, yielding a less dense mesh-like structure, specifically at the oral pole (Fig. 6c,d). In untreated planulae, *Elav1*-positive neurons are elongated in the ectoderm of the oral pole, creating a ‘crown-like’ structure not seen in baclofen-treated planulae. Because the cnidarian nervous system also includes the stinging cells known as cnidocytes, we also analysed genes specifically expressed during cnidogenesis (Fig. 6a). Expression of mini-collagen 3 (*NvNcol-3*), a structural protein in the stinging capsule, was markedly reduced in baclofen-treated planulae, as was that of *NvPaxA*, a member of the homeodomain TF family required for cnidocyte development^{61–64}.

The substantial downregulation of key positive regulators of neural differentiation following baclofen treatment indicated that activation of $GABA_B$ R signalling inhibits neurogenesis. Thus, we expected to find fewer differentiated neurons in baclofen-treated planulae. To test this hypothesis, we performed immunostaining with anti-FMRFamide neuropeptide antibodies^{36,65}. We compared untreated planulae at 4 and 5 dpf to those treated with baclofen

(24 or 48 h). In the early stages, FMRFamide-like immunoreactive positive neurons were found in the ectodermal layer (Fig. 6e–h). As the planulae grew, these neurons formed a net throughout the ectoderm and endoderm with high density in the oral region (Fig. 6i). We detected FMRFamide-like immunoreactive neurons in the ectoderm layer in both control and baclofen-treated planulae. Far fewer of these FMRFamide-like immunoreactive neurons were observed 24 h after baclofen treatment (Fig. 6f,h). Following neural differentiation at 5 dpf, control planulae exhibited neurites connecting the neurons in both the ectoderm and endoderm, as well as the presence of basi-epithelial neurites connecting ectodermal neurons (Fig. 6i,k). By contrast, in 5-dpf planulae following 48 h of baclofen treatment, only a few neurons developed neurites (Fig. 6j,l,m). These results are also supported by transcriptomic analysis of RFamide (Fig. 6n). Hence, we conclude that the $GABA_B$ R signalling pathway inhibits neuron formation and nervous system development in *Nematostella*.

Discussion

In this study, we have demonstrated that sustained activation of $GABA_B$ R by either a specific agonist or a positive allosteric modulator is sufficient to inhibit planula-to-polyp transformation in a reversible and non-toxic manner, while removal of these modulators facilitated continuation of the *Nematostella* developmental plan. Metamorphosis inhibition was previously shown to co-occur with inhibition of apical organ formation^{66,67}. Here, activation of $GABA_B$ R signalling did not affect the apical tuft, but inhibited metamorphosis. Interestingly, in the ascidian *Ciona*, GABA was shown to positively regulate metamorphosis via $GABA_B$ R by inducing GnRH secretion⁶⁸. GABA may also regulate metamorphosis in marine snails, bivalves and sea urchins, although receptors mediating these effects have not been characterized nor have additional GABA signalling components been implicated^{69–71}.

In contrast, we identified four *Nematostella* $GABA_B$ R homologues with all the conserved features of a functional $GABA_{B1}$ R.

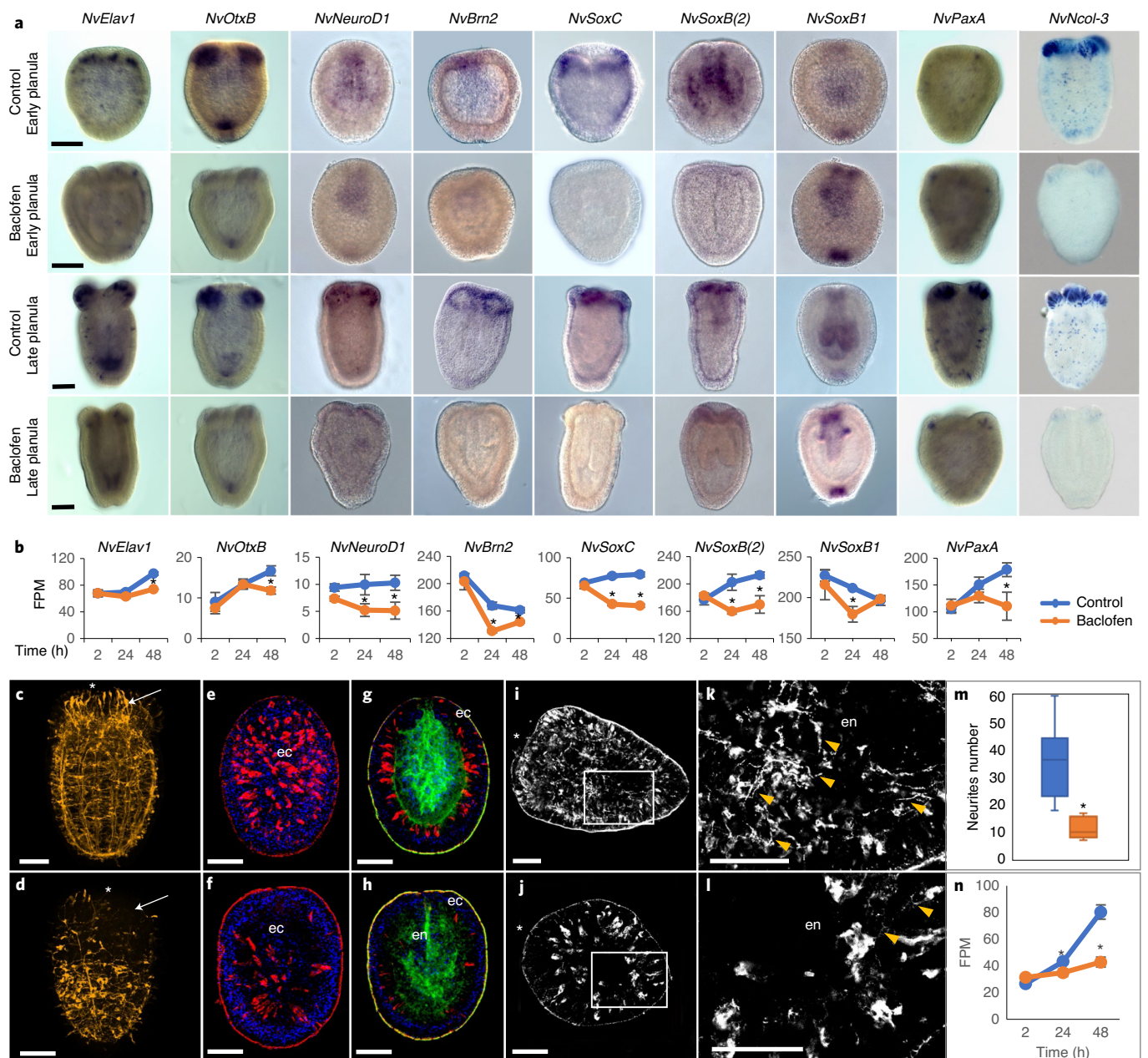


Fig. 6 | Baclofen inhibits *Nematostella* neurogenesis. **a**, Whole-mount in situ hybridization for neurogenesis-related genes in early and late control and baclofen-treated planulae for 24 h (early planulae) and 48 h (late planulae). Images represent 60–91% of the findings from a total of 23–138 planulae per gene. **b**, Transcriptome analysis of significantly (*adjusted $P < 0.005$) differentially expressed neuronal genes (FPM) 2, 24 and 48 h after addition of baclofen and in control planulae. **c, d**, Confocal sections of 6-dpf *NvElav1::mOrange* control (**c**) and baclofen-treated planulae (**d**) labelled with anti-mCherry antibodies. Note the less organized *NvElav1*-expressing neuron net in baclofen-treated planulae, specifically in the oral part (indicated by arrows). Images represent >88% of the findings from 55–60 planulae per treatment. **e–h**, Confocal sections of 4-dpf control (**e, g**) and baclofen-treated planulae (**f, h**) labelled with antibodies against FMRamide (red), phalloidin (green) and DAPI (blue). Surface view of control (**e**) and baclofen treated planulae (**f**). Cross-section through the control planula (**g**) and baclofen-treated planula (**h**). Note in **g** the organization of FMRamide-like immunoreactive neurons in the ectoderm. **i, j**, Confocal sections of 6-dpf control (**i**) and baclofen-treated planulae (**j**) labelled with anti-FMRamide antibodies (white). **k**, Magnification of white rectangle in **i, l**. Magnification of white rectangle in **j**. Note the developed neurites (indicated by yellow arrowheads) in control (**k**) versus baclofen-treated planulae (**l**). **m**, Box plot comparing neurite numbers in control and baclofen-treated planulae ($n = 8$, $P < 0.005$). **n**, Transcriptome analysis of Ramide differentially expressed 2, 24 and 48 h following addition of baclofen and in control planulae. The oral side is facing upward in all images, or labelled with an asterisk. ec, ectoderm; en, endoderm. Scale bars, 50 μm .

Our analysis suggested these proteins have smaller GABA-binding pockets that do not accommodate the larger antagonists for mammalian GABA_BR and, indeed, the latter had no effect on *Nematostella* metamorphosis. Interestingly, in the freshwater cnidarian *Hydra*,

GABA_BR agonists and antagonists were shown to affect the feeding response, although the receptors responsible for this phenotype remain to be characterized^{72,73}. Differences in ligand binding were also found elsewhere, despite the high conservation between

vertebrate and invertebrate GABA_{B1}R homologues. For example, baclofen had no effect in *Drosophila melanogaster* or *C. elegans*, while highly effective antagonists of mammalian GABA_{B1}R had no effect in *Drosophila*^{19,74}.

We also showed a functional connection to broader GABA regulation pathways. Baclofen affected the expression of diverse GABA metabolism enzymes, reducing GABA biosynthesis and transport and increasing GABA removal and degradation, suggesting a functional autoregulated GABA signalling system in *Nematostella*. The finding that several GABA_A receptors were also downregulated following baclofen application supports cross-talk between GABA_B and GABA_A signalling, as suggested in mammalian systems⁷⁵.

In mammals, GABA_BR activation promoted quiescence of neural stem cells and inhibition of neurogenesis^{13,16,17}. Our results show significant downregulation of neural-related TFs, suggesting a specific neural effect of GABA_BR signalling in *Nematostella*. However, a direct effect of GABA on neuronal progenitors remains to be demonstrated, as knockdown technologies are efficient only at early post-fertilization stages and do not persistently reduce genes that are expressed and function at late developmental stages, such as GABA_{B1}R. Other mechanisms, such as inhibition of cell proliferation, increased cell death or specific inhibition of tentacle elongation, could also interfere indirectly with neurogenesis. However, our data do not support any of these alternatives. GABA_BR signalling might inhibit planula cell differentiation, similar to how GABA_BR regulates blood progenitor maintenance in *Drosophila*⁷⁶ or indirectly changes the expression of participating TFs. However, since our findings show downregulation of specific TFs expressed in progenitor/undifferentiated cells, it is tempting to speculate that activation of GABA_BR in *Nematostella* affects neurogenesis by specifically and directly inhibiting the differentiation of undifferentiated cells into neurons.

Since baclofen activation of GABA_BR inhibited pro-neuronal gene expression and neurogenesis, we suggest the involvement of GABA_BR signalling in neurogenesis is evolutionarily conserved between *Nematostella* and higher organisms. The decreases in NvElav1- and FMRamide-like immunoreactive neuron populations and neurite development in baclofen-treated planulae support such inhibition of neuronal developmental programmes. We also found that genes related to cnidocyst synthesis and regulation were downregulated following baclofen treatment, in accord with previous findings in *Hydra* suggesting that GABA_BR plays a role in cnidocyst discharge⁷². Unlike the sustained transcriptomic downregulation of neuron-related genes following the addition of baclofen, NvSoxB1 expression quickly recovered to control levels. In Bilateria the two SoxB family subgroups, SoxB1 and SoxB2, serve antagonistic functions, controlling both neuron stem cell maintenance and neuron differentiation⁷⁷. In vertebrates, SoxB1 genes maintain cells as proliferative precursors and prevent neural differentiation^{78–80} while SoxB2 expression counteracts and represses SoxB1 activity to promote neural differentiation⁸¹. In *Nematostella*, classification of SoxB subgroups remains unclear^{82–84}. While little is known of NvSoxB1 (refs. ^{52,85}), NvSoxB(2) was shown to be required for neuronal progenitor cell development, including that of cnidocytes^{33,86}. Our results support these findings, because baclofen caused downregulation of NvSoxB(2), of downstream genes involved in neurogenesis and of cnidocyte synthesis-related genes. Thus, our findings imply that the continuation of planula development to primary polyps is strongly related to the neurogenesis programme.

Our study thus highlights *Nematostella* as a new model system for investigation of GABA signalling, and opens up new avenues for comparative studies of GABA signalling function and evolution. Furthermore, the rapid and simple developmental cycle of *Nematostella* and the ease of high-throughput screening of modulators establish *Nematostella* as an exciting and simple

model organism for further exploration of the extended GABA signalling pathway.

Methods

Sea anemone culture. Anemones were cultured in *Nematostella* medium (NM), composed of 12.5 ppt artificial sea water (Red Sea) maintained at 18 °C in the dark. Anemones were fed five times per week with freshly hatched *Artemia* brine shrimps⁸⁷. Mature sea anemones were induced to spawn as described previously⁸⁸. Embryos were raised at 21 °C in the dark, and planulae or polyps were collected for experiments.

Pharmacological treatments. Treatments were performed in triplicate, with each plate containing approximately 100 planulae. The GABA_BR agonists GABA (10⁻⁴, 10⁻³ M, Sigma-Aldrich), baclofen (10⁻⁴ M, Sigma-Aldrich) or CGP-7930 (10⁻⁵ M, Sigma-Aldrich)⁸⁸ were added at 3 or 4 dpf. Baclofen and GABA were dissolved in water using NM as control, whereas CGP-7930 was dissolved in DMSO using NM with 10⁻⁵ M DMSO as control. Planulae were raised in the dark at 21 °C. To remove agonists, the medium was replaced five times. To assess the rate of metamorphosis, primary polyps were counted daily. The effect of GABA_BR antagonists on metamorphosis was tested using Phaclofen (10⁻⁴, 10⁻³ M, Sigma-Aldrich) and the high-affinity antagonist CGP 54626 (10⁻⁷, 10⁻⁵ M, Cayman). Muscimol (10⁻⁴ M, Sigma-Aldrich) was used to test whether GABA_AR played a role in metamorphosis.

Identification and cloning of *Nematostella* GABA_BR. To identify *Nematostella* homologues of human GABA_BR, the human GABA_{B1b}R (NP068703) and GABA_{B2}R (CAA09942) sequences served as queries in a blastp search of all *Nematostella* proteins in the NCBI RefSeq database. In addition, we also searched for *Nematostella* homologues with the N-terminal extracellular region and the transmembrane regions of the human queries separately, using both the blastp and tblastn options. Putative homologues identified served as queries against the UniProt database to confirm homology. This search identified eight candidate GABA_BR homologues in *Nematostella*, seven of these genes appearing in a large genomic survey of chemical-transmission-related genes³⁴. Four genes (v1g244104, v1g239821, v1g206093 and v1g243252) had full sequences, and the full-length sequences of the three previously identified³⁴ partial *Nematostella* GABA_BR homologues (v1g86565, v1g158857 and v1g87697) and a newly identified homologue (v1g210496) were PCR amplified using the following primers (with NCBI identifiers): 5', ATGTCAAAGTGTCCGAGCTATTG and 3', TCACTCTTTTGATTGCATCGGAC for NvGABA_{B1a} (MH194577); 5', AGACCAAAGGCCGACTCACAA and 3', TGACAAACCGATATACCGCGA for NvGABA_{B1b} (MH194578); 5', ATGTTCAATATTTCTGTGGCCTGT and 3', CCTTAGTAAATAAATTTATTGGCGAGA for NvGABA_{B1c} (MH194579); and 5', CAGAAATGAACGGCACAAGC and 3', ACGCATGCAAAAATACAATATCTTTT for NvGABA_{B1d} (MH355581), followed by sequencing.

Domain predictions and 3D structural analysis. Putative *Nematostella* GABA_BR genes were translated into proteins using the ExPASy online translate tool (<http://web.expasy.org/translate>). Sequence conservation was visualized using the ExPASy online boxshade tool (http://www.ch.embnet.org/software/BOX_form.html). Conserved domains in *Nematostella* GABA_BR proteins were identified using the consensus predictions of three different databases: the NCBI Conserved Domain Database (<https://www.ncbi.nlm.nih.gov/cdd>), InterPro (<http://www.ebi.ac.uk/interpro>) and SMART (<http://smart.embl-heidelberg.de>). To identify predicted transmembrane regions, we used a consensus of predictions from the servers TMHMM (<http://www.cbs.dtu.dk/services/TMHMM>), TOPCONS (<http://topcons.net>) and SignalP4.1 (<http://www.cbs.dtu.dk/services/SignalP>). Coiled-coil domains were predicted using a consensus of SMART (<http://smart.embl-heidelberg.de>), pcoils (<https://toolkit.tuebingen.mpg.de/#/tools/pcoils>) and Paircoil2-MIT (<http://cb.csail.mit.edu/cb/paircoil2>) predictions.

We generated 3D models of the extracellular regions of NvGABA_BR proteins with SWISS_MODEL (<https://swissmodel.expasy.org>)⁸⁹, using the crystal structure of the extracellular domain of human GABA_BR (PDB ID 4MS4) as template⁵. The C-terminal regions were excluded from the analysis because of low similarity. The following protein data bank (PDB) crystal structures were used for binding site analysis: 4MS3, structure of the extracellular domain of human GABA_BR bound to the endogenous agonist GABA; 4MS4, structure of the extracellular domain of human GABA_BR bound to the agonist baclofen; and 4MR7, structure of the extracellular domain of human GABA_BR bound to the antagonist CGP 54626. Visualization of the 3D models was realized using the PyMOL Molecular Graphics System (<https://pymol.org>).

RNA extraction, sequencing and bioinformatics analysis. Having observed no morphological differences following baclofen treatment at 3 and 4 dpf, transcriptome experiments were conducted at 4 dpf, just before the start of metamorphosis (Fig. 4a). Baclofen-treated (10⁻⁴ M) and control planulae were tested in triplicate at 200 planulae per sample. Samples were taken for RNA extraction from controls and after the addition of baclofen at 2, 24 and 48 h.

In addition, samples of planulae treated with baclofen for 24 h were washed, and collected 2 and 24 h later. Samples were frozen in TriReagent (Sigma-Aldrich) at -80°C . Total RNA was extracted using TriReagent (Sigma-Aldrich) according to the manufacturer's instructions. RNA was further purified using the RNA Clean & Concentrator TM-5 kit (Zymo Research), and genomic DNA residues were removed by DNase treatment (Ambion). RNA quality and concentration were determined using an Agilent 2200 TapeStation.

Groups of 24 samples were prepared for multiplex sequencing using the NEB Ultra Directional RNA kit according to the manufacturer's instructions. Samples were sequenced using 50-base pair single-end reads in two lanes on an Illumina HiSeq2000 and a TruSeq v.3 flow chamber at the Life Sciences and Engineering Infrastructure Centre of the Technion, Haifa, Israel. Illumina reads data were quality filtered and adaptor trimmed using Trimmomatic, with $>95\%$ read survival. Filtered reads (about 12–18 million reads for the different samples) were mapped and quantitated versus the *N. vectensis* genome (NCBI genome GCA_000209225.1), using STAR (v.2.4.2a)⁹⁰. In total, 72–75% of the reads per sample mapped uniquely and 80–85% of these mapped to unique loci. Differential expression analysis was conducted using generalized linear models in DESeq2 (ref. ⁹¹). Specifically, after excluding the six wash samples, we used the design '~ time+treatment+batch+time*condition', which considers the additive effect of three factors, and the interaction between the time and treatment (denoted by an asterisk). For testing of all 24 samples, the interaction term was omitted. DESeq2 normalization was verified using MA plots, and is represented as fragments per kilobase million (FPKM). Comparisons with adjusted $P < 0.05$ were considered significant. Expected factor-dependent trends were verified using nMDS graphs in Vegan (<https://github.com/vegandevs/vegan>) with nMDS stress values ≤ 0.1 , which is considered a close representation of pairwise dissimilarity between objects in a lower dimensional space. Heat maps were generated using shinyheatmap (<http://shinyheatmap.com>)⁹². Illumina results were deposited in the SRA database with accession no. SRP140400. Functional enrichment was conducted with GoSeq⁹³, using the Wallenius bias method, to allow corrections for gene-length biases on differentially expressed significance. A GO non-canonical database for GoSeq was first built using the Ensembl *Nematostella* database, v.45 (metazoa.ensembl.org), and KEGG *Nematostella* (<https://www.genome.jp/kegg/kegg2.html>). For the TF analysis portrayed in Fig. 5e, only TFs with significant expression changes (adjusted $P < 0.05$) were initially selected. Then, only TFs showing cell-type-specific expression (fold change > 1.5 in any cell cluster, as defined in ref. ⁴⁶) were considered. TFs are assigned (colour coded) to the cell cluster with maximum fold change expression.

In situ hybridization and immunohistochemistry. Whole-mount in situ hybridization and immunohistochemistry were performed as previously described^{94,95}. The following primary antibodies were used: anti-GABA (1:500, Abcam, no. ab86186), anti-mCherry (to detect mOrange; 1:200, Abcam, no. ab167453) and anti-FMRamide (Merck Millipore, no. AB15348). The following secondary antibodies were used: donkey anti-mouse Alexa Fluor 488 (Jackson, no. 715-545-150), goat anti-rabbit rhodamine (Jackson, no. 711-295-152) and goat anti-rabbit Alexa Fluor 647 (Jackson, no. 111-605-144). F-actin labelling was performed using Alexa Fluor 488-conjugated phalloidin (2 U ml⁻¹ 66 nM, Sigma-Aldrich), and nuclear staining was performed with DAPI (1:1,000, Sigma-Aldrich).

Microscopy and imaging. In situ hybridization was visualized using a Zeiss Axio Imager 2 epifluorescence microscope equipped with an AxioCam MRm camera (Carl Zeiss). Immunofluorescence was visualized by confocal microscopy (Nikon, C1-SHS UMT). Planulae were visualized using a Nikon binocular (Multizoom Az-100) or Nikon eclipse Ti microscope. Images were captured and quantified using NIS-element software (Nikon). Relative comparisons used the same settings and exposures for all captured images. All images were assembled without adjustment of contrast or brightness. For quantification of neurite numbers, an area of $210 \times 210 \mu\text{m}^2$ from eight planulae was analysed.

Reporting Summary. Further information on research design is available in the Nature Research Reporting Summary linked to this article.

Data availability

Transcriptome datasets used in this study are available via the SRA database with accession no. SRP140400.

Received: 1 October 2019; Accepted: 29 September 2020;

Published online: 09 November 2020

References

- Ulrich, D. & Bettler, B. GABA_B receptors: synaptic functions and mechanisms of diversity. *Curr. Opin. Neurobiol.* **17**, 298–303 (2007).
- Kaupmann, K. et al. GABA B-receptor subtypes assemble into functional heteromeric complexes. *Nature* **396**, 683–687 (1998).
- Jones, K. A. et al. GABA_B receptors function as a heteromeric assembly of the subunits GABA_BR1 and GABA_BR2. *Nature* **396**, 674–679 (1998).
- White, J. H. et al. Heterodimerization is required for the formation of a functional GABA B receptor. *Nature* **396**, 679–682 (1998).
- Geng, Y., Bush, M., Mosyak, L., Wang, F. & Fan, Q. R. Structural mechanism of ligand activation in human GABA_B receptor. *Nature* **504**, 254–259 (2013).
- Galvez, T. et al. Mutagenesis and modeling of the GABA_B receptor extracellular domain support a venus flytrap mechanism for ligand binding. *J. Biol. Chem.* **274**, 13362–13369 (1999).
- Margeta-Mitrovic, M., Jan, Y. N. & Jan, L. Y. A trafficking checkpoint controls GABA_B receptor heterodimerization. *Neuron* **27**, 97–106 (2000).
- Robbins, M. J. et al. GABA_{B2} is essential for G-protein coupling of the GABA_B receptor heterodimer. *J. Neurosci.* **21**, 8043–8052 (2001).
- Kniazeff, J., Galvez, T., Labesse, G. & Pin, J. P. No ligand binding in the GB2 subunit of the GABA(B) receptor is required for activation and allosteric interaction between the subunits. *J. Neurosci.* **22**, 7352–7361 (2002).
- Liu, J. et al. Molecular determinants involved in the allosteric control of agonist affinity in the GABA_B receptor by the GABA_{B2} subunit. *J. Biol. Chem.* **279**, 15824–15830 (2004).
- Felder, C. B., Graul, R. C., Lee, A. Y., Merkle, H. P. & Sadee, W. The Venus flytrap of periplasmic binding proteins: an ancient protein module present in multiple drug receptors. *AAPS PharmSciTech.* **1**, 7–26 (1999).
- Kilb, W., Kirischuk, S. & Luhmann, H. Role of tonic GABAergic currents during pre- and early postnatal rodent development. *Front. Neural Circuits* **7**, 139 (2013).
- Fukui, M. et al. Modulation of cellular proliferation and differentiation through GABA_B receptors expressed by undifferentiated neural progenitor cells isolated from fetal mouse brain. *J. Cell. Physiol.* **216**, 507–519 (2008).
- Gaiarsa, J.-L., Kuczewski, N. & Porcher, C. Contribution of metabotropic GABA_B receptors to neuronal network construction. *Pharmacol. Ther.* **132**, 170–179 (2011).
- Bony, G. et al. Non-hyperpolarizing GABA_B receptor activation regulates neuronal migration and neurite growth and specification by cAMP/LKB1. *Nat. Commun.* **4**, 1800 (2013).
- Giachino, C. et al. GABA suppresses neurogenesis in the adult hippocampus through GABA_B receptors. *Development* **141**, 83–90 (2014).
- Sibbe, M. & Kulik, A. GABAergic regulation of adult hippocampal neurogenesis. *Mol. Neurobiol.* **54**, 5497–5510 (2017).
- Dittman, J. S. & Kaplan, J. M. Behavioral impact of neurotransmitter-activated G-protein-coupled receptors: muscarinic and GABA_B receptors regulate *Caenorhabditis elegans* locomotion. *J. Neurosci.* **28**, 7104–7112 (2008).
- Mezler, M., Müller, T. & Raming, K. Cloning and functional expression of GABA_B receptors from *Drosophila*. *Eur. J. Neurosci.* **13**, 477–486 (2001).
- Colombo, G. (ed.) *GABA_B Receptor Vol. 29* (Springer, 2016).
- Blankenburg, S. et al. Cockroach GABA_B receptor subtypes: molecular characterization, pharmacological properties and tissue distribution. *Neuropharmacology* **88**, 134–144 (2015).
- Rentzsch, F., Layden, M. & Manuel, M. The cellular and molecular basis of cnidarian neurogenesis. *Wiley Interdiscip. Rev. Dev. Biol.* **6**, e257 (2016).
- Ryan, J. F. & Chiodin, M. Where is my mind? How sponges and placozoans may have lost neural cell types. *Phil. Trans. R. Soc. B* **370**, 20150059 (2015).
- Nickel, M. Evolutionary emergence of synaptic nervous systems: what can we learn from the non-synaptic, nerveless Porifera? *Invertebr. Biol.* **129**, 1–16 (2010).
- Watanabe, H. in *Brain Evolution by Design: From Neural Origin to Cognitive Architecture* (eds Shigeno, S. et al.) 45–75 (Springer Japan, 2017).
- Moroz, L. L. & Kohn, A. B. Independent origins of neurons and synapses: insights from ctenophores. *Phil. Trans. R. Soc. Lond. B* **371**, 20150041 (2016).
- Kelava, I., Rentzsch, F. & Technau, U. Evolution of eumetazoan nervous systems: insights from cnidarians. *Phil. Trans. R. Soc. Lond. B* **370**, 20150065 (2015).
- Galliot, B. & Quiquand, M. A two-step process in the emergence of neurogenesis. *Eur. J. Neurosci.* **34**, 847–862 (2011).
- Layden, M. J., Rentzsch, F. & Röttinger, E. The rise of the starlet sea anemone *Nematostella vectensis* as a model system to investigate development and regeneration. *Wiley Interdiscip. Rev. Dev. Biol.* **5**, 408–428 (2016).
- Rentzsch, F., Juliano, C. & Galliot, B. Modern genomic tools reveal the structural and cellular diversity of cnidarian nervous systems. *Curr. Opin. Neurobiol.* **56**, 87–96 (2019).
- Rentzsch, F. & Technau, U. Genomics and development of *Nematostella vectensis* and other anthozoans. *Curr. Opin. Genet. Dev.* **39**, 63–70 (2016).
- Putnam, N. et al. Sea anemone genome reveals ancestral eumetazoan gene repertoire and genomic organization. *Science* **317**, 86–94 (2007).
- Darling, J. A. et al. Rising starlet: the starlet sea anemone, *Nematostella vectensis*. *Bioessays* **27**, 211–221 (2005).
- Ancil, M. Chemical transmission in the sea anemone *Nematostella vectensis*: a genomic perspective. *Comp. Biochem. Physiol. D* **4**, 268–289 (2009).
- Bosch, T. C. G. et al. Back to the basics: cnidarians start to fire. *Trends Neurosci.* **40**, 92–105 (2017).

36. Marlow, H. Q., Srivastava, M., Matus, D. Q., Rokhsar, D. & Martindale, M. Q. Anatomy and development of the nervous system of *Nematostella vectensis*, an anthozoan cnidarian. *Dev. Neurobiol.* **69**, 235–254 (2009).
37. Faltine-Gonzalez, D. Z. & Layden, M. J. Characterization of nAChRs in *Nematostella vectensis* supports neuronal and non-neuronal roles in the cnidarian–bilaterian common ancestor. *EvoDevo* **10**, 27 (2019).
38. Adams, C. & Lawrence, A. CGP7930: a positive allosteric modulator of the GABA_B receptor. *CNS Drug Rev.* **13**, 308–316 (2007).
39. Lee, P. N., Pang, K., Matus, D. Q. & Martindale, M. Q. A. WNT of things to come: evolution of Wnt signaling and polarity in cnidarians. *Semin. Cell Dev. Biol.* **17**, 157–167 (2006).
40. Trevino, M., Stefanik, D. J., Rodriguez, R., Harmon, S. & Burton, P. M. Induction of canonical Wnt signaling by alsterpaullone is sufficient for oral tissue fate during regeneration and embryogenesis in *Nematostella vectensis*. *Dev. Dyn.* **240**, 2673–2679 (2011).
41. Kusserow, A. et al. Unexpected complexity of the Wnt gene family in a sea anemone. *Nature* **433**, 156–160 (2005).
42. Gurevich, V. V. & Gurevich, E. V. How and why do GPCRs dimerize? *Trends Pharmacol. Sci.* **29**, 234–240 (2008).
43. Calver, A. R. et al. The C-terminal domains of the GABA_B receptor subunits mediate intracellular trafficking but are not required for receptor signaling. *J. Neurosci.* **21**, 1203–1210 (2001).
44. Grünewald, S. et al. Importance of the γ -aminobutyric acid B receptor C-termini for G-protein coupling. *Mol. Pharmacol.* **61**, 1070–1080 (2002).
45. Pagano, A. et al. C-terminal interaction is essential for surface trafficking but not for heteromeric assembly of GABA_B receptors. *J. Neurosci.* **21**, 1189–1202 (2001).
46. Seb e-Pedr os, A. et al. Cnidarian cell type diversity revealed by whole-organism single-cell RNA-seq analysis. *Cell* **173**, 1520–1534 (2018).
47. Karabulut, A., He, S., Chen, C.-Y., McKinney, S. A. & Gibson, M. C. Electroporation of short hairpin RNAs for rapid and efficient gene knockdown in the starlet sea anemone, *Nematostella vectensis*. *Dev. Biol.* **448**, 7–15 (2019).
48. He, S. et al. An axial Hox code controls tissue segmentation and body patterning in *Nematostella vectensis*. *Science* **361**, 1377–1380 (2018).
49. Benke, D. in *Advances in Pharmacology* (ed. Blackburn, T. P.) 93–111 (Elsevier, 2010).
50. Kantamneni, S. et al. GISP binding to TSG101 increases GABA_B receptor stability by down-regulating ESCRT-mediated lysosomal degradation. *J. Neurochem.* **107**, 86–95 (2008).
51. Kantamneni, S., Holman, D., Wilkinson, K. A., Nishimune, A. & Henley, J. M. GISP increases neurotransmitter receptor stability by down-regulating ESCRT-mediated lysosomal degradation. *Neurosci. Lett.* **452**, 106–110 (2009).
52. Magje, C., Pang, K. & Martindale, M. Genomic inventory and expression of Sox and Fox genes in the cnidarian *Nematostella vectensis*. *Dev. Genes Evol.* **215**, 618–630 (2005).
53. Richards, G. S. & Rentzsch, F. Transgenic analysis of a SoxB gene reveals neural progenitor cells in the cnidarian *Nematostella vectensis*. *Development* **141**, 4681–4689 (2014).
54. Layden, M. J., Boekhout, M. & Martindale, M. Q. *Nematostella vectensis* *achaete-scute* homolog *NvashA* regulates embryonic ectodermal neurogenesis and represents an ancient component of the metazoan neural specification pathway. *Development* **139**, 1013–1022 (2012).
55. Richards, G. S. & Rentzsch, F. Regulation of *Nematostella* neural progenitors by SoxB, Notch and bHLH genes. *Development* **142**, 3332–3342 (2015).
56. Layden, M. J. et al. MAPK signaling is necessary for neurogenesis in *Nematostella vectensis*. *BMC Biol.* **14**, 61 (2016).
57. Watanabe, H. et al. Sequential actions of β -catenin and Bmp pattern the oral nerve net in *Nematostella vectensis*. *Nat. Commun.* **5**, 5536 (2014).
58. Mazza, M. E., Pang, K., Martindale, M. Q. & Finnerty, J. R. Genomic organization, gene structure, and developmental expression of three clustered otx genes in the sea anemone *Nematostella vectensis*. *J. Exp. Zool. B* **308**, 494–506 (2007).
59. Nakanishi, N., Renfer, E., Technau, U. & Rentzsch, F. Nervous systems of the sea anemone *Nematostella vectensis* are generated by ectoderm and endoderm and shaped by distinct mechanisms. *Development* **139**, 347–357 (2012).
60. Marlow, H., Roettinger, E., Boekhout, M. & Martindale, M. Q. Functional roles of Notch signaling in the cnidarian *Nematostella vectensis*. *Dev. Biol.* **362**, 295–308 (2012).
61. Babonis, L. S. & Martindale, M. Q. *PaxA*, but not *PaxC*, is required for cnidocyte development in the sea anemone *Nematostella vectensis*. *EvoDevo* **8**, 14 (2017).
62. Zenkert, C., Takahashi, T., Diesner, M.-O. &  zbek, S. Morphological and molecular analysis of the *Nematostella vectensis* cnidom. *PLoS ONE* **6**, e22725 (2011).
63. Sunagar, K. et al. Cell type-specific expression profiling unravels the development and evolution of stinging cells in sea anemone. *BMC Biol.* **16**, 108 (2018).
64. Matus, D. Q., Pang, K., Daly, M. & Martindale, M. Q. Expression of *Pax* gene family members in the anthozoan cnidarian, *Nematostella vectensis*. *Evol. Dev.* **9**, 25–38 (2007).
65. Zatylny-Gaudin, C. & Favrel, P. Diversity of the RFamide peptide family in mollusks. *Front. Endocrinol. (Lausanne)* **5**, 178 (2014).
66. Bause, M., van der Horst, R. & Rentzsch, F. Glypican1/2/4/6 and sulfated glycosaminoglycans regulate the patterning of the primary body axis in the cnidarian *Nematostella vectensis*. *Dev. Biol.* **414**, 108–120 (2016).
67. Rentzsch, F., Fritzenwanker, J. H., Scholz, C. B. & Technau, U. FGF signalling controls formation of the apical sensory organ in the cnidarian *Nematostella vectensis*. *Development* **135**, 1761–1769 (2008).
68. Hozumi, A. et al. GABA-Induced GnRH release triggers chordate metamorphosis. *Curr. Biol.* **30**, 1555–1561 (2020).
69. Biscocho, D., Cook, J. G., Long, J., Shah, N. & Leise, E. M. GABA is an inhibitory neurotransmitter in the neural circuit regulating metamorphosis in a marine snail. *Dev. Neurobiol.* **78**, 736–753 (2018).
70. Joyce, A. & Vogeler, S. Molluscan bivalve settlement and metamorphosis: neuroendocrine inducers and morphogenetic responses. *Aquaculture* **487**, 64–82 (2018).
71. Rahmani, M. & Uehara, T. Induction of metamorphosis and substratum preference in four sympatric and closely related species of sea urchins (Genus *Echinometra*) in Okinawa. *Zool. Stud.* **40**, 29–43 (2001).
72. Scappaticci, A. A. & Kass-Simon, G. NMDA and GABA_B receptors are involved in controlling nematocyst discharge in hydra. *Comp. Biochem. Physiol. A* **150**, 415–422 (2008).
73. Lauro, B. M. & Kass-Simon, G. Hydra's feeding response: effect of GABA_B ligands on GSH-induced electrical activity in the hypostome of *H. vulgaris*. *Comp. Biochem. Physiol. A* **225**, 83–93 (2018).
74. Schaeffer, J. M. & Hsueh, A. J. Identification of gamma-aminobutyric acid and its binding sites in the rat ovary. *Life Sci.* **30**, 1599–1604 (1982).
75. Shen, W., Nan, C., Nelson, P. T., Ripps, H. & Slaughter, M. M. GABA_B receptor attenuation of GABA_A currents in neurons of the mammalian central nervous system. *Physiol. Rep.* **5**, e13129 (2017).
76. Shim, J. et al. Olfactory control of blood progenitor maintenance. *Cell* **155**, 1141–1153 (2013).
77. Sarkar, A. & Hochedlinger, K. The Sox family of transcription factors: versatile regulators of stem and progenitor cell fate. *Cell Stem Cell* **12**, 15–30 (2013).
78. Bylund, M., Andersson, E., Novitch, B. G. & Muhr, J. Vertebrate neurogenesis is counteracted by Sox1–3 activity. *Nat. Neurosci.* **6**, 1162–1168 (2003).
79. Pevny, L. & Placzek, M. SOX genes and neural progenitor identity. *Curr. Opin. Neurobiol.* **15**, 7–13 (2005).
80. Wegner, M. SOX after SOX: SOXession regulates neurogenesis. *Genes Dev.* **25**, 2423–2428 (2011).
81. Whittington, N., Cunningham, D., Le, T.-K., De Maria, D. & Silva, E. M. Sox21 regulates the progression of neuronal differentiation in a dose-dependent manner. *Dev. Biol.* **397**, 237–247 (2015).
82. Royo, J. L. et al. Transphyletic conservation of developmental regulatory state in animal evolution. *Proc. Natl Acad. Sci. USA* **108**, 14186–14191 (2011).
83. Jager, M., Qu innec, E., Le Guyader, H. & Manuel, M. Multiple Sox genes are expressed in stem cells or in differentiating neuro-sensory cells in the hydrozoan *Clytia hemisphaerica*. *EvoDevo* **2**, 12 (2011).
84. Schnitzler, C. E., Simmons, D. K., Pang, K., Martindale, M. Q. & Baxevas, A. D. Expression of multiple Sox genes through embryonic development in the ctenophore *Mnemiopsis leidyi* is spatially restricted to zones of cell proliferation. *EvoDevo* **5**, 15 (2014).
85. Steinmetz, P. R. H., Aman, A., Kraus, J. E. M. & Technau, U. Gut-like ectodermal tissue in a sea anemone challenges germ layer homology. *Nat. Ecol. Evol.* **1**, 1535–1542 (2017).
86. Busengdal, H. & Rentzsch, F. Unipotent progenitors contribute to the generation of sensory cell types in the nervous system of the cnidarian *Nematostella vectensis*. *Dev. Biol.* **431**, 59–68 (2017).
87. Elran, R. et al. Early and late response of *Nematostella vectensis* transcriptome to heavy metals. *Mol. Ecol.* **23**, 4722–4736 (2014).
88. Fritzenwanker, J. & Technau, U. Induction of gametogenesis in the basal cnidarian *Nematostella vectensis* (Anthozoa). *Dev. Genes Evol.* **212**, 99–103 (2002).
89. Bordoli, L. et al. Protein structure homology modeling using SWISS-MODEL workspace. *Nat. Protoc.* **4**, 1–13 (2008).
90. Dobin, A. et al. STAR: ultrafast universal RNA-seq aligner. *Bioinformatics* **29**, 15–21 (2013).
91. Love, M. I., Huber, W. & Anders, S. Moderated estimation of fold change and dispersion for RNA-seq data with DESeq2. *Genome Biol.* **15**, 506 (2014).
92. Khomtchouk, B. B., Hennessy, J. R. & Wahlestedt, C. shinyheatmap: ultra fast low memory heatmap web interface for big data genomics. *PLoS ONE* **12**, e0176334 (2017).
93. Young, M. D., Wakefield, M. J., Smyth, G. K. & Oshlack, A. Gene ontology analysis for RNA-seq: accounting for selection bias. *Genome Biol.* **11**, R14 (2010).

94. Wolenski, F. S., Layden, M. J., Martindale, M. Q., Gilmore, T. D. & Finnerty, J. R. Characterizing the spatiotemporal expression of RNAs and proteins in the starlet sea anemone, *Nematostella vectensis*. *Nat. Protoc.* **8**, 900–915 (2013).
95. Genikhovich, G. & Technau, U. Anti-acetylated tubulin antibody staining and phalloidin staining in the starlet sea anemone *Nematostella vectensis*. *Cold Spring Harb. Protoc.* **2009**, pdb.prot5283 (2009).
96. Gassmann, M. & Bettler, B. Regulation of neuronal GABA_B receptor functions by subunit composition. *Nat. Rev. Neurosci.* **13**, 380–394 (2012).

Acknowledgements

We thank F. Rentzsch for providing the *NvElav1* reporter line. We thank the Bioinformatics Service Unit at the University of Haifa and, specifically, N. Sher and M. Lalzar for their assistance. We thank S. Ben-Tabou de-Leon for helpful comments. This work was supported by the Israel Ministry of Science and Technology (grant no. 3-8774), the Israel Science Foundation (grant nos. 1454/13, 2155/15 and 3512/19) and the DS Research Centre at the University of Haifa.

Author contributions

S.L. designed and performed experiments. V.B. performed gene cloning, shRNA knockdown and assisted in experiments. S.L., A.B. and M.K. performed sequence and structure analysis. A.M. performed bioinformatics analyses. A.S.-P. analysed GABA_BR

homologue and TF expression in the single-cell dataset. S.L., V.B., M.K. and T.L. analysed the data. M.K. supervised sequence and structure analysis. T.L. conceived and supervised the project and wrote the manuscript with M.K. and input from all authors. All authors discussed the results and commented on the manuscript. All authors read and approved the final version of the manuscript.

Competing interests

The authors declare no competing interests.

Additional information

Extended data is available for this paper at <https://doi.org/10.1038/s41559-020-01338-3>.

Peer review information *Nature Ecology & Evolution* thanks the anonymous reviewers for their contribution to the peer review of this work.

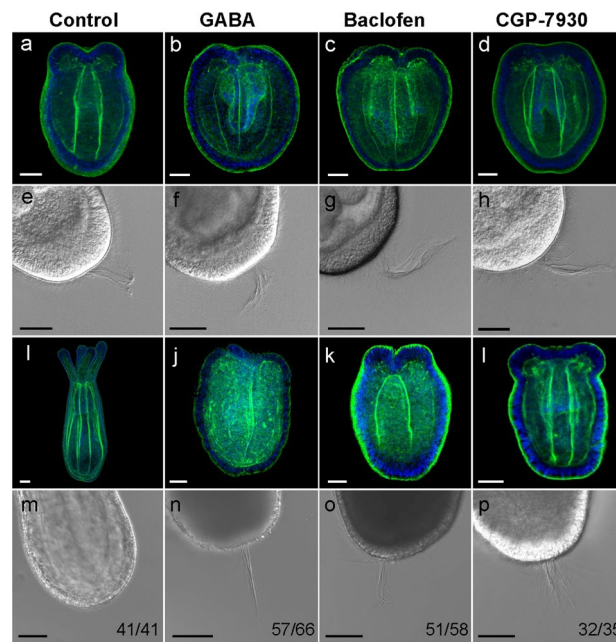
Supplementary information is available for this paper at <https://doi.org/10.1038/s41559-020-01338-3>.

Correspondence and requests for materials should be addressed to M.K. or T.L.

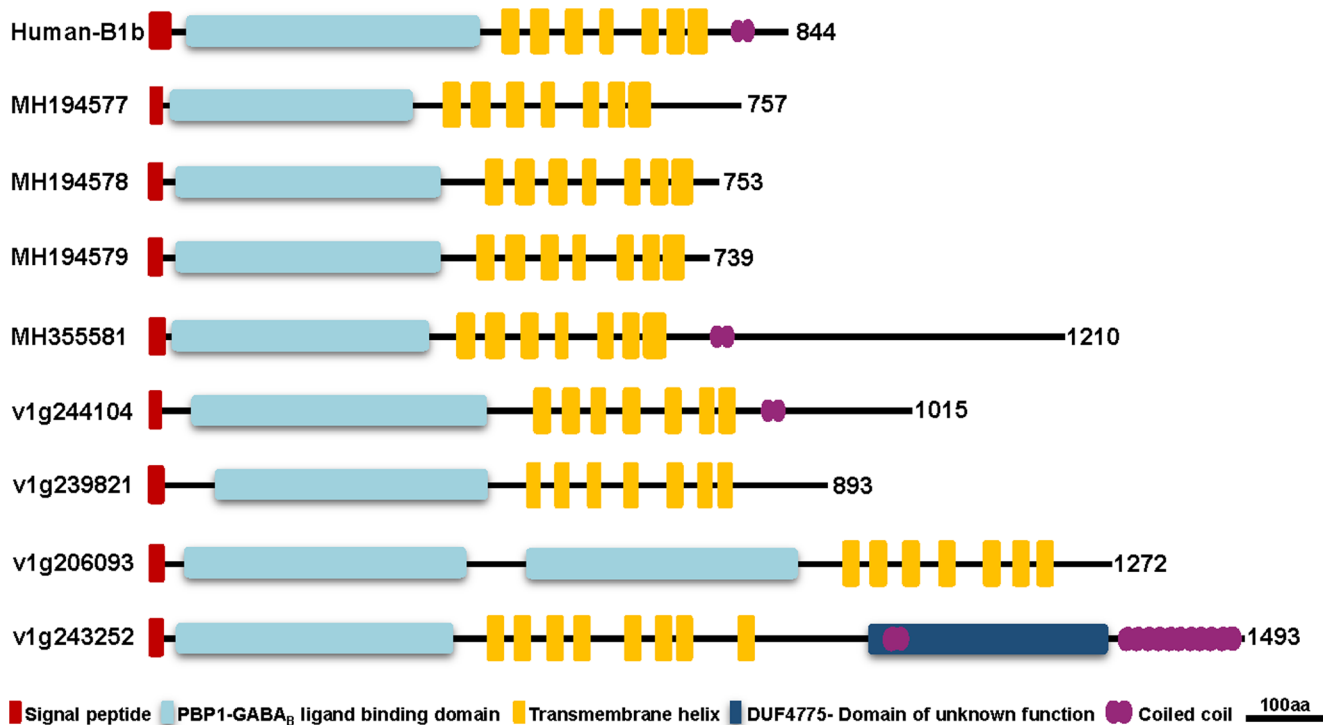
Reprints and permissions information is available at www.nature.com/reprints.

Publisher's note Springer Nature remains neutral with regard to jurisdictional claims in published maps and institutional affiliations.

© The Author(s), under exclusive licence to Springer Nature Limited 2020



Extended Data Fig. 1 | GABA_BR modulators inhibit planulae-to-polyp transformation. Confocal sections at 5 dpf (a-d) and 8 dpf (i-l) labeled with antibodies against phalloidin (green) and DAPI (blue). DIC images of the aboral/apical tuft at 5 dpf (e-h) and 8 dpf (m-p). Control planulae (a,i) and primary polyps (i, m) are shown, as are planulae treated with GABA (b, f, j, n), baclofen (c, g, k, o) or CGP-7930 (d, h, l, p). While at 5 dpf all planulae possessed an apical tuft (numbers are not shown), in 8 dpf control primary polyps after metamorphosis (m), the apical tuft was lost, whereas treated 8 dpf planulae (n-p) still maintained it. The fraction of similar phenotypes from the total number of analyzed samples is given in the lower right-hand corner. Scale bars, 50 μ m.



Extended Data Fig. 2 | Schematic representation of predicted domains in putative *Nematostella* GABA_BR homologs in comparison to human GABA_BR. The eight *Nematostella* proteins contain a conserved signal peptide, an extracellular 'Periplasmic Binding Protein type1 (PBP1) GABA_B ligand-binding domain' (the structural VFT module that in mammals binds GABA), predicted helical transmembrane domains, and coiled-coil domains. One *Nematostella* homolog (v1g206093) contained two extracellular domains, each corresponding to a separate predicted VFT module. These two domains are 26% identical in sequence, suggesting that they serve dissimilar functions (Supplementary Fig. 2). v1g243252 contains eight predicted TM helices and a -300 residue domain of unknown function (DUF4475) located after these TM domains. However, the intracellular C-terminal domains of the *Nematostella* homologs present low similarity to the corresponding regions of human sequences. Coiled-coil motifs found in the C-terminus of human GABA_BR were predicted in three *Nematostella* homologs. The mammalian GABA_BR C-terminal domain mediate processes such as trafficking out of the ER or modulation of receptor activity⁴⁴, but it has also been suggested as non-essential for functional GABA_BR heterodimers^{42,43,45}. GABA_BR C-termini therefore differ dramatically between mammals and cnidarians, suggesting they do not affect essential functions, and were excluded from the full comparison. Protein domains were predicted as detailed in Methods.

Reporting Summary

Nature Research wishes to improve the reproducibility of the work that we publish. This form provides structure for consistency and transparency in reporting. For further information on Nature Research policies, see [Authors & Referees](#) and the [Editorial Policy Checklist](#).

Statistics

For all statistical analyses, confirm that the following items are present in the figure legend, table legend, main text, or Methods section.

n/a Confirmed

- The exact sample size (n) for each experimental group/condition, given as a discrete number and unit of measurement
- A statement on whether measurements were taken from distinct samples or whether the same sample was measured repeatedly
- The statistical test(s) used AND whether they are one- or two-sided
Only common tests should be described solely by name; describe more complex techniques in the Methods section.
- A description of all covariates tested
- A description of any assumptions or corrections, such as tests of normality and adjustment for multiple comparisons
- A full description of the statistical parameters including central tendency (e.g. means) or other basic estimates (e.g. regression coefficient) AND variation (e.g. standard deviation) or associated estimates of uncertainty (e.g. confidence intervals)
- For null hypothesis testing, the test statistic (e.g. F , t , r) with confidence intervals, effect sizes, degrees of freedom and P value noted
Give P values as exact values whenever suitable.
- For Bayesian analysis, information on the choice of priors and Markov chain Monte Carlo settings
- For hierarchical and complex designs, identification of the appropriate level for tests and full reporting of outcomes
- Estimates of effect sizes (e.g. Cohen's d , Pearson's r), indicating how they were calculated

Our web collection on [statistics for biologists](#) contains articles on many of the points above.

Software and code

Policy information about [availability of computer code](#)

Data collection

No software was used.

Data analysis

Conserved domains were identified using the consensus of three different databases: the NCBI Conserved Domain Database (<https://www.ncbi.nlm.nih.gov/cdd>), InterPro (<http://www.ebi.ac.uk/interpro>) and SMART (<http://smart.embl-heidelberg.de>). To identify predicted transmembrane regions, we used a consensus among the servers TMHMM (<http://www.cbs.dtu.dk/services/TMHMM>), TOPCONS (<http://topcons.net>) and SignalP4.1 (<http://www.cbs.dtu.dk/services/SignalP>). Coiled-coil domains were predicted using a consensus of SMART (<http://smart.embl-heidelberg.de>), pcoils (<https://toolkit.tuebingen.mpg.de/#/tools/pcoils>) and Paircoil2-MIT (<http://cb.csail.mit.edu/cb/paircoil2>). 3D models were generated using Swiss-model (<https://swissmodel.expasy.org>) and were visualized using the PyMOL Molecular Graphics System (<https://pymol.org>). Illumina reads were quality-filtered and adapter-trimmed using Trimmomatic, and inspected with Fastqc (www.bioinformatics.babraham.ac.uk). Filtered reads were mapped and quantitated using STAR (version 2.4.2a). Differential expression analysis was conducted using DESeq2. For more details see Methods.

For manuscripts utilizing custom algorithms or software that are central to the research but not yet described in published literature, software must be made available to editors/reviewers. We strongly encourage code deposition in a community repository (e.g. GitHub). See the Nature Research [guidelines for submitting code & software](#) for further information.

Data

Policy information about [availability of data](#)

All manuscripts must include a [data availability statement](#). This statement should provide the following information, where applicable:

- Accession codes, unique identifiers, or web links for publicly available datasets
- A list of figures that have associated raw data
- A description of any restrictions on data availability

Transcriptome datasets used in this study are available via the SRA database with accession no. SRP140400.

Field-specific reporting

Please select the one below that is the best fit for your research. If you are not sure, read the appropriate sections before making your selection.

Life sciences Behavioural & social sciences Ecological, evolutionary & environmental sciences

For a reference copy of the document with all sections, see [nature.com/documents/nr-reporting-summary-flat.pdf](https://www.nature.com/documents/nr-reporting-summary-flat.pdf)

Life sciences study design

All studies must disclose on these points even when the disclosure is negative.

Sample size	<input type="text" value="Not applicable"/>
Data exclusions	<input type="text" value="No data exclusions"/>
Replication	<input type="text" value="All replications were successful"/>
Randomization	<input type="text" value="Not applicable"/>
Blinding	<input type="text" value="Not applicable"/>

Reporting for specific materials, systems and methods

We require information from authors about some types of materials, experimental systems and methods used in many studies. Here, indicate whether each material, system or method listed is relevant to your study. If you are not sure if a list item applies to your research, read the appropriate section before selecting a response.

Materials & experimental systems

n/a	Involvement in the study
<input type="checkbox"/>	<input checked="" type="checkbox"/> Antibodies
<input checked="" type="checkbox"/>	<input type="checkbox"/> Eukaryotic cell lines
<input checked="" type="checkbox"/>	<input type="checkbox"/> Palaeontology
<input type="checkbox"/>	<input checked="" type="checkbox"/> Animals and other organisms
<input checked="" type="checkbox"/>	<input type="checkbox"/> Human research participants
<input checked="" type="checkbox"/>	<input type="checkbox"/> Clinical data

Methods

n/a	Involvement in the study
<input checked="" type="checkbox"/>	<input type="checkbox"/> ChIP-seq
<input checked="" type="checkbox"/>	<input type="checkbox"/> Flow cytometry
<input checked="" type="checkbox"/>	<input type="checkbox"/> MRI-based neuroimaging

Antibodies

Antibodies used	<input type="text" value="anti-GABA , anti-mCherry , anti-FMRamide"/>
Validation	<input type="text" value="These antibodies are commonly used and were reported in previous publications."/>

Animals and other organisms

Policy information about [studies involving animals](#); [ARRIVE guidelines](#) recommended for reporting animal research

Laboratory animals	<input type="text" value="Nematostella vectensis"/>
Wild animals	<input type="text" value="Not applicable"/>
Field-collected samples	<input type="text" value="Not applicable"/>
Ethics oversight	<input type="text" value="No ethical approval is needed (invertebrate)"/>

Note that full information on the approval of the study protocol must also be provided in the manuscript.